






# Optimization of tungsten inert gas welding process parameters for joining austenitic stainless steel and copper using the Taguchi method

Nabil Bensaid<sup>1\*</sup> , Mohamed Farid Benlamnour<sup>1</sup> , Yazid Laib Dit Laksir<sup>2</sup> ,  
Tahar Saadi<sup>1</sup> , Riad Badji<sup>1</sup> 

<sup>1</sup> Research Center in Industrial Technologies (CRTI), PB 64, Chéraga, Algiers, Algeria

<sup>2</sup> Department of Mechanical Engineering, University of L'Arbi Ben M'hidi, Oum el Bouaghi, Algeria

\* Corresponding author's e-mail: nblbensaid@gmail.com

## ABSTRACT

This study aims to optimize the tungsten inert gas (TIG) welding parameters for joining AISI 316L stainless steel and Cu-ETP copper using 309L stainless steel filler rods. Welding dissimilar materials is challenging due to their significant differences in thermal and mechanical properties. The high thermal conductivity of Cu-ETP copper leads to rapid heat dissipation, causing uneven heat distribution at the weld interface. To address this issue, the research team applied a 1 mm offset of the welding torch toward the copper side to balance the heat input. They employed statistical analyses using ANOVA and the Taguchi method to determine the optimal process parameters. The results showed that the optimal welding current, welding speed, and gas flow for achieving high tensile strength ( $R_m$ ) are 90 A, 0.5 mm/s, and 12 l/min, respectively. Among these, welding speed emerged as the most significant factor, influencing 48.74% of the weld characteristics. Mechanical testing confirmed that these parameters produced high-quality welds. Metallurgical analysis revealed minimal diffusion between the materials, preserving their distinct properties while minimizing the formation of undesirable intermetallic phases. These results highlight the effectiveness of TIG welding in creating robust joints between AISI 316L stainless steel and Cu-ETP copper for applications requiring a combination of both materials' properties.

**Keywords:** TIG welding, optimization, Taguchi method, stainless steel, ANOVA, copper, mechanical properties, metallurgical characterization.

## INTRODUCTION

Welding is a widely recognized manufacturing process that enables the permanent joining of similar or dissimilar materials, typically through the application of heat. A filler material, which may or may not match the base materials, is often used to facilitate this process [1–3]. Over the years, welding technology has advanced significantly, driven by its extensive industrial applications. While joining similar materials is relatively straightforward, welding dissimilar materials presents unique difficulties due to differences in metallurgical, chemical, and thermal properties. Despite these complexities, the potential benefits, such as cost savings and weight reduction, make

dissimilar welding highly attractive in various industrial sectors, including automotive, aerospace, and shipbuilding, where each metal component offers distinct advantages [4, 5].

To address these difficulties, various welding techniques have been developed. Solid-state methods like friction welding and friction stir welding offer benefits such as reduced heat-affected zones, high joint strength, and the elimination of solidification cracking [6]. However, these techniques often require specialized equipment and involve technical complexities that limit their widespread adoption. As a result, fusion-welding processes like TIG welding continue to be actively researched due to their versatility and broad application range. The performance of welded components in these

processes depends heavily on the precise selection of process parameters, such as welding current, welding speed, gas flow rate, and electrode diameter. Traditionally, these parameters have been determined through trial and error or based on welder experience, approaches that can be both time-consuming and resource-intensive [7, 8].

To improve the efficiency of parameter selection, several optimization methods have been explored. Techniques such as genetic algorithms and response surface methodology offer comprehensive solutions for multi-objective optimization. However, the Taguchi method stands out for its simplicity, efficiency, and proven effectiveness in optimizing single-objective problems. This method reduces the number of experimental trials required, saving time and resources, while providing a structured framework to identify the most influential factors and their optimal levels. Additionally, the use of the signal-to-noise (S/N) ratio enhances the robustness of the results, making the Taguchi method particularly suitable for initial process optimization. For more complex scenarios requiring the optimization of multiple characteristics, the Taguchi approach can be effectively supplemented with techniques like grey relational analysis, balancing simplicity, resource efficiency, and adaptability [9, 10].

Welding dissimilar materials, such as copper and stainless steel, is particularly complex and poses unique challenges due to their vastly different physical, chemical, and thermal properties. Copper’s high thermal conductivity leads to rapid heat dissipation, making it difficult to reach the necessary melting temperature and creating a thermal imbalance at the joint interface. This issue is exacerbated when welding materials with contrasting characteristics, resulting in uneven heat distribution. Precise control over welding parameters is therefore essential to achieve strong, defect-free joints [11, 12].

The welding of stainless steel to copper holds substantial industrial importance, particularly in the production of thermal equipment, such as heat exchangers, where the distinct thermal and mechanical properties of these two materials are essential [13]. Due to their excellent corrosion

resistance and capacity to withstand significant temperature fluctuations, stainless steel-copper assemblies are widely employed in sectors such as energy, chemical, and food processing industries [14]. However, achieving these welds presents a technical challenge due to the significant thermophysical differences between the two materials, especially regarding thermal expansion coefficients and conductivities [15].

In this context, our study focuses on optimizing TIG welding parameters to enhance the quality of stainless steel-copper joints, aiming to meet the increasing industrial demands for performance, durability, and reliability.

## MATERIALS AND METHODS

### Process and materials

The materials used in this study comprised 3-mm-thick sheets of Cu-ETP copper and AISI 316L austenitic stainless steel. The choice of these materials provides significant advantages due to their complementary properties: AISI 316L offers excellent corrosion resistance and high ductility, making it suitable for applications requiring durability and flexibility, while Cu-ETP copper has superior electrical and thermal conductivity, essential for efficient heat dissipation [16, 17] (Table 1).

However, welding these dissimilar materials presents challenges due to their differing physical and thermal properties. To address these issues, TIG welding was selected for its precise heat input control, critical when joining materials with contrasting thermal conductivities, such as copper and stainless steel. TIG welding minimizes the risk of overheating, distortion, and defects, resulting in clean, strong welds with excellent fusion and high-quality joints, crucial for applications demanding durability and precision [18–20]. To enhance the bond between the dissimilar materials, 1.5 mm diameter 309L stainless steel filler rods, an austenitic stainless steel, were used for their complementary properties, ensuring weld strength and reliability under the study’s demanding conditions.

**Table 1.** Chemical composition of AISI 316L ASS base material and 309 filler metal

Element.	C	Cr	Ni	Mo	Si	Mn
AISI 316 L	0.003	17.01	10.31	2.03	0.61	1.53
309 Filler	0.19	22.25	14.15	0.13	0.46	1.89

Pure argon (99.99%) served as the protective gas. Specific adjustments, such as offsetting the welding torch by 1 mm toward the copper side, were made to achieve a more balanced heat input and enhance weld quality. Figure 1 illustrates the weld appearance of the joints, highlighting smooth surfaces with minimal defects, like porosity or undercuts, indicating proper fusion. The uniform weld bead demonstrates the effectiveness of the optimized TIG welding parameters in achieving balanced heat distribution between AISI 316L stainless steel and Cu-ETP copper (Table 2).

### Selection of output and input parameters

The selection of the experimental conditions was based on mathematically validated Taguchi matrices, which were crucial for optimizing the welding parameters. This optimization ensured not only precise and consistent welding results but also maintained the mechanical integrity of dissimilar joints between copper and stainless steel, in line with ASME standards [21, 22]. Key welding factors, such as welding speed, welding current, and gas flow rate, were chosen due to their critical influence on heat input and joint quality in these dissimilar metal welds.

Based on the Taguchi design, we established the specific numerical combinations shown in Table 3. The minimum and maximum values of these combinations were derived from inert gas tungsten arc welding (TIG) experiments, ensuring defect-free welds. These values were carefully selected based on previous experiments, as discussed in Section 2 (experimental techniques),

**Table 3.** Welding parameters and their levels

Parameters	Level 1	Level 2	Level 3
Speed (mm/s)	0.5	1.5	2.5
Welding current (A)	80	90	100
Gas flow rate (l/min)	8	10	12

to guarantee welded joints free of visible defects. This approach allows us to more accurately assess the influence of welding parameters on tensile strength, without interference from variables related to weld imperfections.

### Taguchi method

The Taguchi method consists of a set of algebraic, mathematical, and statistical techniques for modeling and analyzing technical problems where the response is influenced by various factors. In this study, the Taguchi method was applied to analyze the relationship between welding process parameters and mechanical strength, focusing on how these parameters affect the results. This allows us to create mathematical models to predict the maximum tensile strength  $\sigma_m$  (MPa) based on the welding parameters.

The data necessary for Taguchi analysis was obtained using an L9 orthogonal array design, with three numerical values for each factor across three levels [23]. This experimental design included 9 welding experiments, as detailed in Table 4.

Minitab software was used to analyze the mechanical tensile strength response and to create an experimental model that fits the collected data. The adequacy of this mathematical model was



**Figure 1.** The appearances of the joints

**Table 2.** Chemical composition of Cu-ETP copper

Element	Cu	Bi	O	Pb
% by mass	99.90	0.0005	0.0040	0.0005

**Table 4.** L9 orthogonal array

Experiments	TIG parameters			Rm (MPa)
	Speed (mm/s)	Welding current (A)	Gas flow rate (l/min)	
1	2,5	80	8	166.320
2	2,5	90	10	181.461
3	2,5	100	12	205.112
4	1,5	80	10	193.180
5	1,5	90	12	231.541
6	1,5	100	8	200.156
7	0,5	80	12	215.881
8	0,5	90	8	215.455
9	0,5	100	10	208.756

verified through analysis of variance (ANOVA) and the evaluation of the signal-to-noise (S/N) ratio. The S/N ratio is crucial for determining the optimal combination of welding parameters to achieve the best mechanical response, which was selected based on the criterion that a higher ranking is better. The S/N ratio was calculated using the following equation [24, 25]:

$$S/N = -10 \log \left[ \frac{1}{n} \sum_{k=1}^n \frac{1}{y_k^2} \right] \quad (1)$$

In the equation above, *n* represents the number of repetitions of the experiments, while *a* denotes the performance value of experiment *k*. Based on this, the average signal-to-noise ratio is calculated for each level of the welding factors, with the optimal level identified as the one having the highest signal-to-noise ratio for each level of the welding parameters.

Analysis of variance (ANOVA) is conducted to assess the significance of the process parameters. Statistical analysis of variance is crucial for identifying the parameters that significantly influence welding performance. This analysis involves calculating the total sum of squares of deviations from the overall mean of the response performance indicator, determining the ratios of these deviations, and evaluating the experimental error. Typically, the significance level for ANOVA is set at 95%, meaning that parameters with a p-value less than 0.05 are considered statistically significant for the welding factor being assessed.

### Mechanical testing

To apply the Taguchi design in this study (Table 4), the welding process (TIG) was performed with a single pass, following ASME standards

[22]. Throughout the welding process, parameters such as current, argon flow rate, and feed speed were systematically varied across the welded sheets to explore their effects. The mechanical properties of the dissimilar welded joints were evaluated later through tensile testing in accordance with ASTM-E8 standards [26]. Standard tensile samples were prepared and tested using the SATEC INSTRON tensile testing machine, which operates at a strain rate of 0.1 per second.

### RESULTS

To determine the welding process parameters that significantly affect tensile strength, analysis of variance (ANOVA) was conducted on the response performance indicator. The significance of each parameter is determined by the F-value, as shown in the ANOVA tables (Tables 5–7), with the analysis performed at a 95% confidence level. Welding parameters are considered significant if they have a p-value less than 0.05, indicating their impact on the quality and performance of dissimilar welds.

The three tables (Tables 5–7) are essential for analyzing the experimental results and assessing the impact of the process parameters on performance. Table 5 presents the analysis of variance for the signal-to-noise ratio, examining the differences in signal-to-noise ratios based on the welding parameter values. This analysis helps improve performance by maximizing the signal-to-noise ratio according to the specified criteria. Table 6 contains the analysis of variance for the means, evaluating the effects of parameter levels on the average values of the measured responses and identifying the parameters that significantly affect these means. Finally, Table 7 summarizes the

**Table 5.** Analysis of variance for signal-to-noise ratio

Source	DF	Seq SS	Adj SS	Adj MS	F	P
Speed	2	28878.11	28878.11	14439.06	0.731	0.527
Welding current	2	9906.11	9906.11	4953.06	0.251	0.787
Gas flow rate	2	20456.44	20456.44	10228.22	0.518	0.625

**Table 6.** Analysis of variance for means

Source	DF	Seq SS	Adj SS	Adj MS	F	P
Speed	2	144882	144882	72441.0	0.717	0.533
Welding current	2	50274	50274	25137.0	0.249	0.789
Gas flow rate	2	108150	108150	54075.0	0.535	0.616

**Table 7.** Response table for signal-to-noise ratios

Level	Speed	Welding current	Gas flow rate
1	213.4	191.8	194.0
2	208.3	209.5	194.5
3	184.3	204.7	217.5
Delta	29.1	17.7	23.5
Rank	1	3	2

signal-to-noise ratio values for each parameter group, allowing for direct comparison of relative performance to select the optimal configuration. Together, these tables provide a systematic approach to process improvement by identifying the critical parameters that influence the mechanical resistance of dissimilar welds.

Table 5 shows that the welding factor with the most significant difference (rank 1) among the levels is speed, confirming that it has the most substantial effect on tensile strength compared to other welding factors. This aligns with the previous ANOVA analysis, which indicated that speed has the largest impact. In contrast, gas also shows a noticeable difference (rank 2) among the levels. The current shows the smallest difference (rank 3) between the levels, suggesting that it has the least effect on the response variable, consistent with the ANOVA results where current did not exhibit a significant impact. Based on ANOVA analysis, it found that the impact percentages of welding current, welding speed and gas flow on  $R_m$  are, respectively, 16.72%, 48.74%, and 34.54%.

Figures 2 and 3 illustrate the main effects plots for the signal-to-noise (S/N) ratios and the averages, demonstrating how welding factors affect these measures either positively or negatively. The S/N ratio plots reveal that the best results are achieved at a lower speed of 0.5 mm/s and a high gas flow

rate of 12, using a current of 90 amps. Similarly, for the averages, a comparable trend is observed: a speed of 0.5 mm/s and a gas flow rate of 12 yield the highest values, with a current of 90 amps providing optimal performance. Therefore, to ensure high tensile strength, it is advisable to select a lower speed, a moderate current, and a high gas flow rate.

By using Minitab 21, a regression model for tensile strength can be created based on the welding factors, modeling the relationship between mechanical resistance ( $R_m$ ) and the parameters of welding speed, welding current, and gas flow rate with a general linear equation as follows:

$$R_m = a + b \times Speed + c \times Current + d \times Gas \quad (2)$$

where:  $a$ : is the intercept,  $b$ ,  $c$ , and  $d$ : are the coefficients for speed, current, and gas flow, respectively.

The coefficients  $b$ ,  $c$  and  $d$  indicate the effects of welding, current, and gas flow rate on  $R_m$ . Positive or negative values show the direction of the impact, while the magnitude reflects its strength.

According to ANOVA analysis, the values of the coefficients corresponding to  $a$ ,  $b$ ,  $c$ , and  $d$  are as follows: 106.99, -14.53, 0.64 and +0.64. Thus, the previous equation is as follows:

$$R_m = 106.99 - 14.53 \times Speed + 0.64 \times Current + 5.88 \times Gas \quad (3)$$



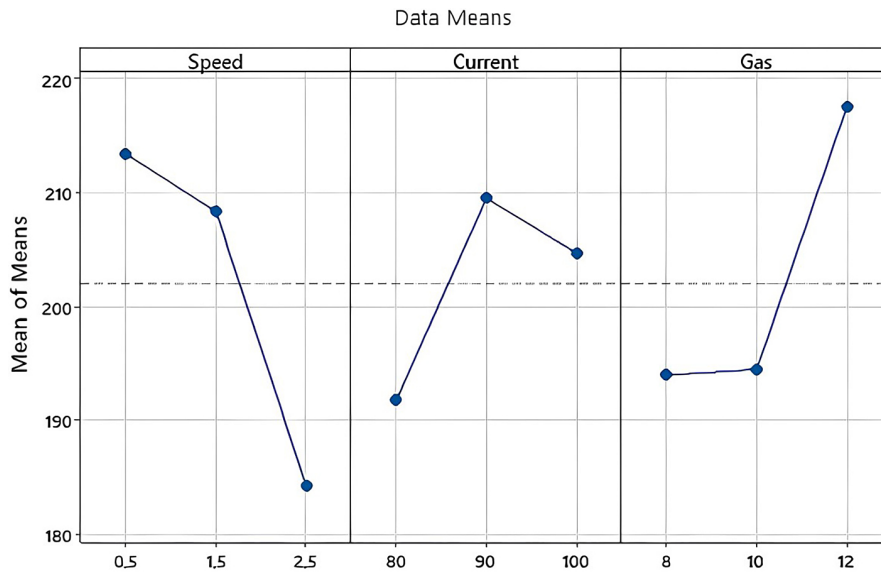


Figure 2. Main effects plot for means

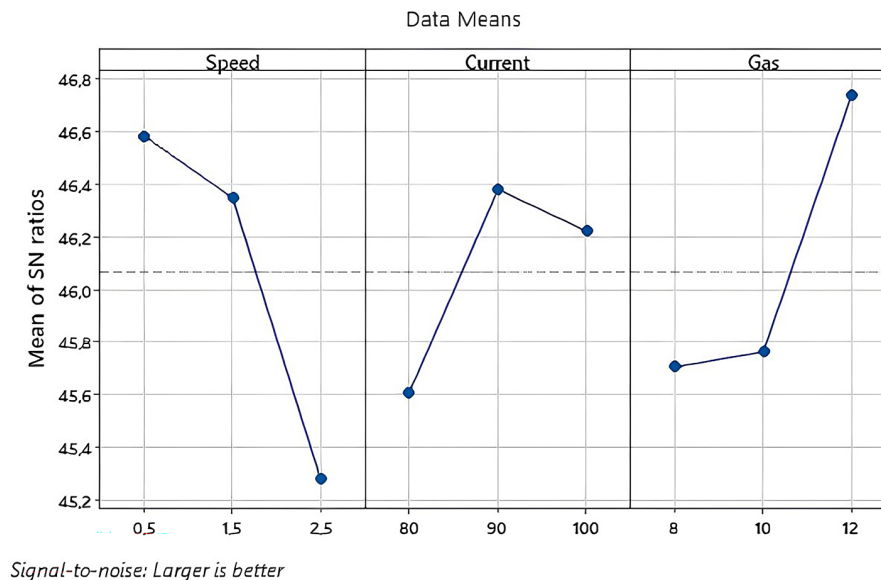


Figure 3. Main effects plot for SN

The model’s coefficient of determination ( $R^2$ ) reaches 0.76, indicating that these parameters explain 76% of the variation in  $R_m$ . The analysis confirms significant predictors with p-values below 0.05. The adjusted  $R^2$  ( $R^2$  adj) is 0.62, which shows that some of the predictor values for tensile strength may not significantly contribute to explaining the true values of  $R_m$ . Therefore, the linear equation accounts for about 62% of the variability in mechanical strength ( $R_m$ ). Figures 4 and 5 illustrate the contour plots of tensile strength ( $R_m$ ) as a function of both speed and gas flow rate (Figure 4), and welding speed and welding current (Figure 5), graphically depicting the relationships

between these variables. In both figures, the major and minor ranges of tensile strength can be inferred, with contour lines or color gradients indicating different levels of  $R_m$ . These plots reveal the variations in  $R_m$  resulting from changes in welding speed and gas flow rate (Figure 4) or welding speed and welding current (Figure 5).

These contour plots are valuable tools for identifying optimal combinations of welding speed and gas flow or welding current to achieve the desired tensile strength, highlighting areas where  $R_m$  changes significantly or gradually. Additionally, they reveal interactions between speed and other process parameters, aiding in the

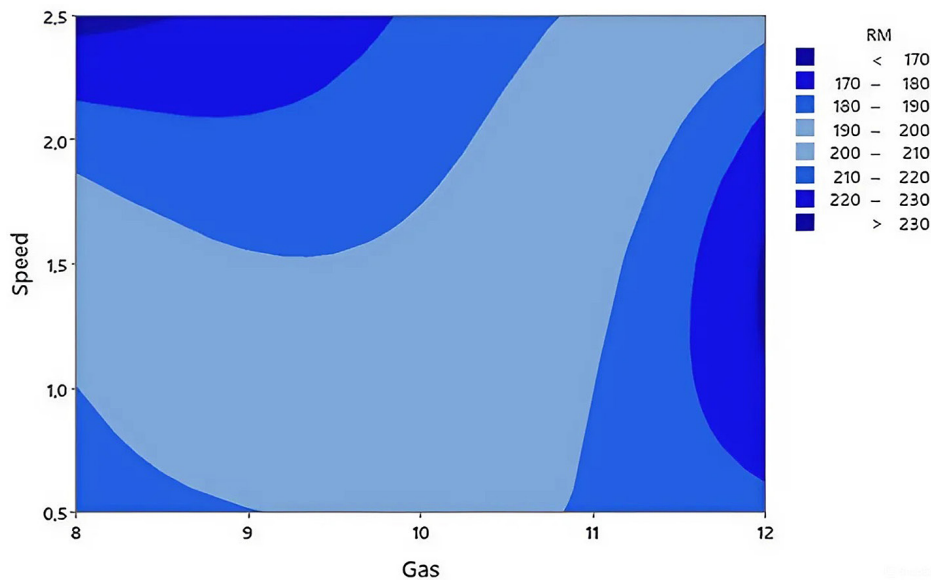


Figure 4. Contour plot of  $R_m$  as function of speed and gas

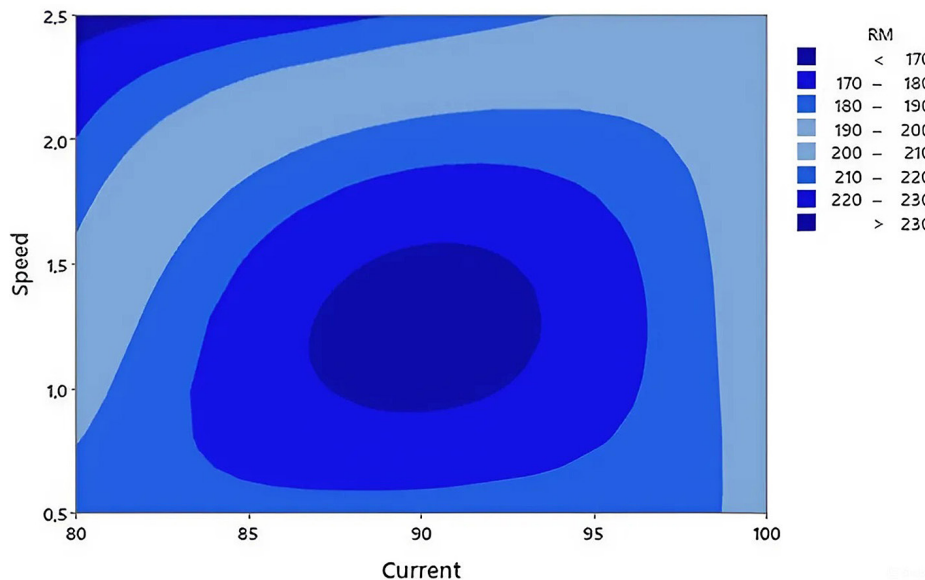


Figure 5. Contour plot of  $R_m$  as function of speed and current

optimization of welding conditions for improved mechanical properties.

Figures 6 and 7 present three-dimensional plots that offer deeper insights into the variation of tensile strength ( $R_m$ ) as a function of welding factors. Figure 6 features a three-dimensional representation of speed (x-axis), gas flow rate (y-axis), and tensile strength (z-axis), illustrating the impact of simultaneous changes in welding speed and gas flow on  $R_m$ , while highlighting the minimum and maximum peaks of tensile strength. Similarly, Figure 7 displays a surface plot of  $R_m$  as a function of welding speed and welding current, with the axes representing speed, current, and tensile strength,

respectively. This visualization is essential for understanding the combined effects of welding speed and welding current on  $R_m$  and for identifying parameter combinations that yield either the highest or the lowest tensile strength.

Together, these plots serve as important tools for optimizing process parameters to achieve the desired mechanical properties. They provide clear insights into how these factors interact, enabling informed decisions to enhance the quality of dissimilar welds. Additionally, they can guide future research toward exploring the effects of additional welding factors or developing new techniques in the welding process.

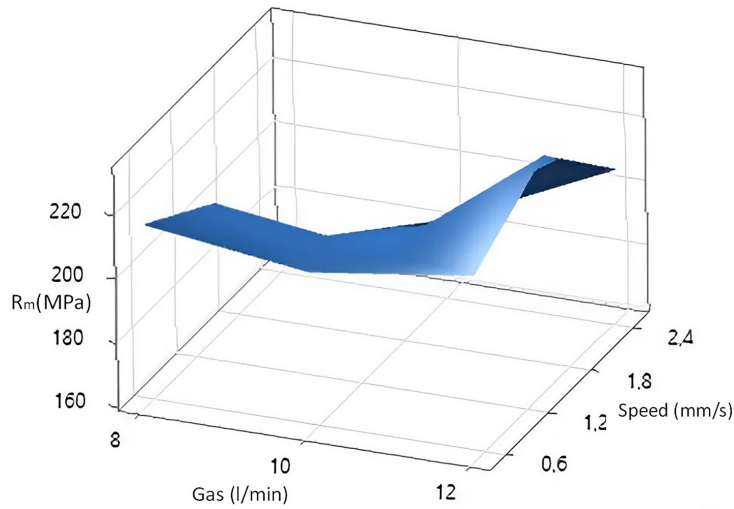


Figure 6. Surface plot of Rm as function of speed and gas

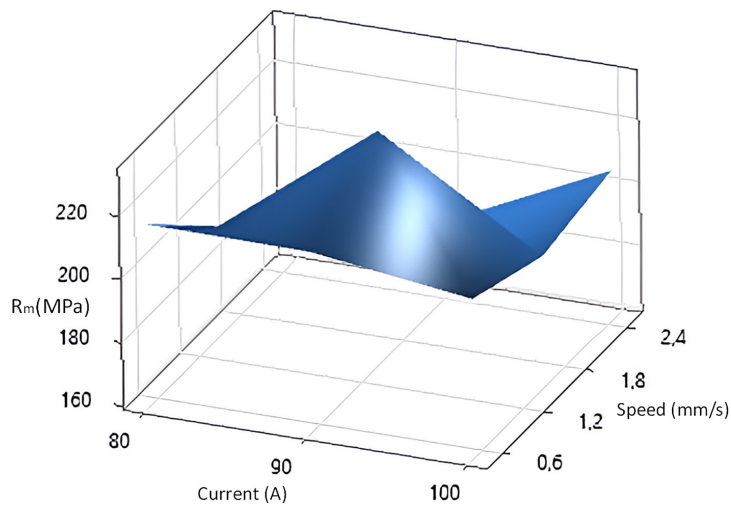


Figure 7. Surface plot of Rm as function of speed and current

### Metallurgical analyses

The microstructure and morphology of the weld interface are critical in TIG welding, as they reflect the intricate interplay of various factors within the welding process. Physical properties, in particular, play a significant role in shaping the thermal, mechanical, and metallurgical conditions at the interface. This complexity is further heightened in dissimilar joining, where the challenge of metallurgical compatibility must be addressed in addition to the inherent phenomena of the process. Understanding the contribution of each material becomes even more crucial in such scenarios, as each one brings unique physical and mechanical properties to the interface. This complexity is well illustrated by the copper-stainless steel interface, as shown in Figure 8. Here, a distinct boundary between the two metals is clearly

visible, with copper on one side and stainless steel on the other. The stainless steel side reveals a relatively homogeneous grain structure, punctuated by subtle discontinuities. These discontinuities are likely the result of residual stresses, which arise due to the different thermal expansion rates of copper and stainless steel. As the weld cools, these mismatches in contraction induce mechanical stresses, particularly in the stainless steel, leading to the formation of these microstructural irregularities. On the copper side, the structure is more uniform, reflecting copper’s high thermal conductivity, which facilitates rapid heat dissipation during welding. This rapid cooling prevents excessive melting or mixing with the stainless steel, resulting in a well-maintained and distinct interface with minimal diffusion across the boundary during the welding process [27, 28].



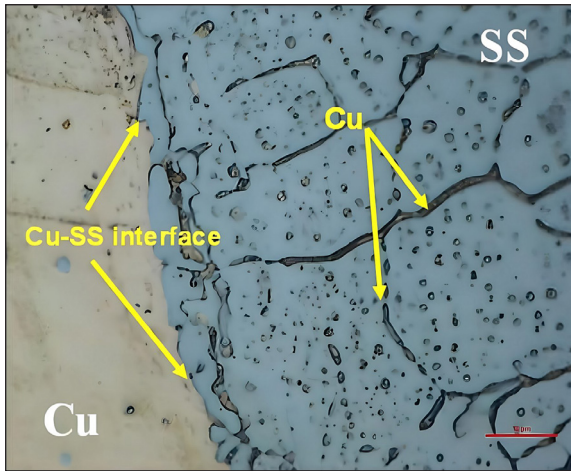


Figure 8. Microstructure of copper-stainless steel interface

To further elucidate these observations, Figure 9 presents the EDX analysis of the interface, which confirms the elemental distribution and interaction between the two metals. The analysis shows that chromium, iron, and nickel are predominantly concentrated on the stainless steel side, with only limited diffusion into the copper region. This limited diffusion is crucial, as it preserves the stainless steels composition even under high welding temperatures. On the copper side, EDX confirms that copper remains primarily within its domain, with negligible migration into the stainless steel.

However, the slight diffusion of nickel toward the copper region correlates with some interaction at the interface. While this interaction does not lead to significant intermetallic phase formation, copper does infiltrate the subtle discontinuities in the stainless steel by diffusion, further stabilizing the weld. The EDX analysis supports the microstructural evidence, confirming that the weld maintains the distinct properties of both metals while ensuring a robust and reliable joint.

### CONCLUSIONS

The goal of this study was to optimize TIG welding parameters for dissimilar welding between AISI 316L stainless steel and Cu-ETP copper. The key findings are as follows:

- Statistical analysis using ANOVA analyses of the Taguchi method showed that the impact percentages of welding current, welding speed, and gas flow on the tensile strength ( $R_m$ ) were 16.72%, 48.74%, and 34.54%, respectively.
- The results indicated that the optimal welding parameters are a welding speed of 0.5 mm/s, a welding current of 90 A, and a gas flow rate of 12 l/min. Furthermore, offsetting the welding torch by 1 mm toward the copper side contributed to achieving a more balanced heat input, resulting in high-quality welds.

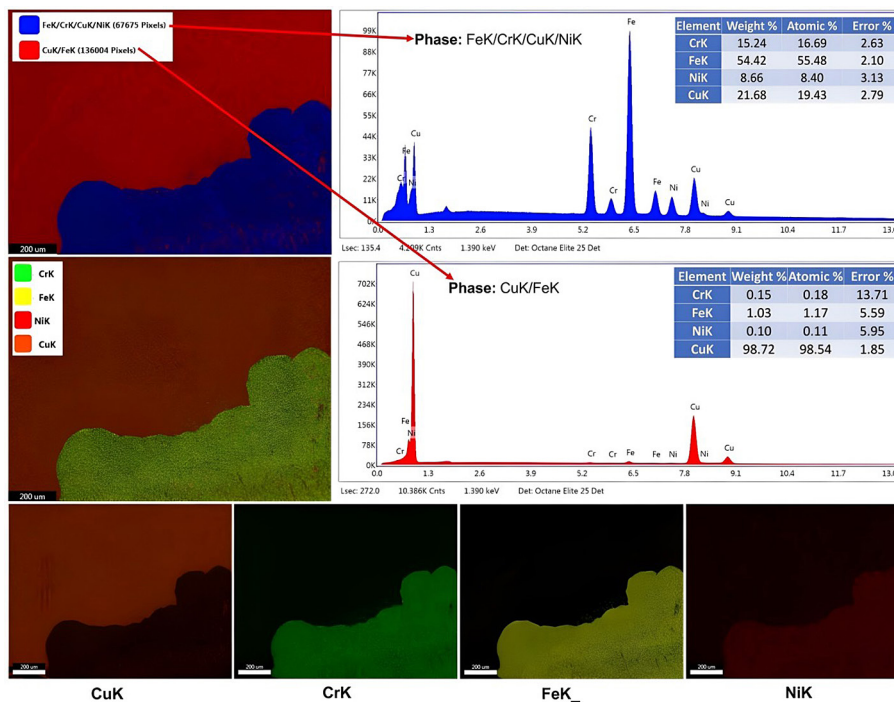


Figure 9. Elemental distribution of the copper-stainless steel interface via EDS mapping

- Metallurgical analysis revealed minimal diffusion between AISI 316L stainless steel and Cu-ETP copper, preserving the distinct properties of both materials and minimizing the formation of intermetallic phases.

This study demonstrates that optimizing TIG welding parameters for dissimilar materials like AISI 316L stainless steel and Cu-ETP copper produces mechanically robust joints while maintaining the unique properties of each material. These findings open up possibilities for applications that leverage the advantages of both materials.

For future research, it would be valuable to explore alternative filler metal alloys to further enhance joint strength and durability, especially in applications exposed to extreme temperatures or corrosive environments. Such work could contribute to improved weld quality and reliability in demanding industrial settings.

## REFERENCES

1. Razzaq S., Pan Z.X., Li H.J., Ringer S.P., Liao X.Z. Joining dissimilar metals by additive manufacturing: A review. *J. Mater. Res. Technol.* 2024, 31, 2820–2845. <https://doi.org/10.1016/j.jmrt.2024.07.033>
2. Abed Al Kareem SS, Mahdi BL, Hussein HK. Impact of TIG welding parameters on the mechanical properties of 6061-T6 aluminum alloy joints. *Advances in Science and Technology Research Journal.* 2023, 17(5), 114–29. <https://doi.org/10.12913/22998624/171489>
3. Conte, R., Battista, F.R., Ambrogio, G. Submerged arc welding process: enhancement of production performance based on metallurgical observations. *Int J Adv Manuf Technol* 2024, 134, 781–793. <https://doi.org/10.1007/s00170-024-14153-y>
4. Benlamouar M.F., Bensaid N., Saadi T., Badji R. Multi-objective optimization and evolution of dissimilar welding process between Cr-Mo steel and austenitic stainless steel for power plant application. *Mater. Res. Express* 2024, 11(2), 026507. <https://doi.org/10.1088/2053-1591/ad28d2>
5. Tong L.G., Gu J.C., Yin S.W., Wang L., Bai S.W. Impacts of torch moving on phase change and fluid flow in weld pool of SMAW. *Int J Heat Mass Transf.* 2016, 100, 949–957. <https://doi.org/10.1016/j.ijheatmasstransfer.2016.04.032>
6. Deepati AK, Alhazmi W, Zakri W, Shaban E, Biswas P. Parametric analysis on the progression of mechanical properties on FSW of aluminum-copper plates. *Advances in Science and Technology Research Journal.* 2022, 16(2), 168–78. <https://doi.org/10.12913/22998624/147123>
7. Kilic S., Ozturk F., Demirdogen M.F. A comprehensive literature review on friction stir welding: Process parameters, joint integrity, and mechanical properties. *J. Eng. Res.* 2023. <https://doi.org/10.1016/j.jer.2023.09.005>
8. Saadi T., Benlamouar M.F., Bensaid N., Boutaghane A., Soualili M.A., Hachemi H. Optimization of automatic TIG welding parameters of AISI 304L ASS welds using response surface methodology. *DDF* 2021, 406, 319–333. <https://doi.org/10.4028/www.scientific.net/ddf.406.319>
9. Mojaver P., Khalilarya S., Chitsaz A., Assadi M. Multi-objective optimization of a power generation system based SOFC using Taguchi/AHP/TOPSIS triple method. *Sustain. Energy Technol. Assess.* 2020, 38, 100674. <https://doi.org/10.1016/j.seta.2020.100674>
10. Li J., Hu J., Cao L., Wang S., Liu H., Zhou Q. Multi-objective process parameters optimization of SLM using the ensemble of metamodells. *J. Manuf. Process.* 2021, 68, Part A, 198–209. <https://doi.org/10.1016/j.jmapro.2021.05.038>
11. Abtan AA, Mohammed MS, Alshahal I. Microstructure, mechanical properties, and heat distribution ANSYS model of CP copper and 316 stainless steel torch brazing. *Advances in Science and Technology Research Journal.* 2024, 18(1), 167–83. <https://doi.org/10.12913/22998624/177299>
12. Vyas H.D., Mehta K.P., Badheka V., Doshi B. Microstructure evolution and mechanical properties of continuous drive friction welded dissimilar copper-stainless steel pipe joints. *Mater. Sci. Eng. A.* 2022, 832, 142444. <https://doi.org/10.1016/j.msea.2021.142444>
13. Cheng Z., Huang J., Ye Z., Chen Y., Yang J., Chen S. Microstructures and mechanical properties of copper-stainless steel butt-welded joints by MIG-TIG double-sided arc welding. *J. Mater. Process. Technol.* 2019, 265, 87–98. <https://doi.org/10.1016/j.jmatprotec.2018.10.007>
14. Zhu L., Zhou Q., Song C., Liu L., Zhang L., Fan K., Zhang Y., Lu H., Hu Q., Sheng Z., Guo Y., Liu K. Microstructure and mechanical properties of T2 copper/316L stainless steel explosive welding composite with small size wavy interface. *J. Mater. Res. Technol.* 2024, 28, 668–682. <https://doi.org/10.1016/j.jmrt.2023.12.031>
15. Ciou Y.C., Chang C.L., Lu W.H., Lin H.K. Mechanical and microstructural properties of dissimilar copper and stainless-steel butt welds prepared using zigzag and circular fiber laser oscillation methods. *Mater. Sci. Eng. A.* 2022, 859, 144178. <https://doi.org/10.1016/j.msea.2022.144178>
16. Mohamed M.A., Manurung Y.H., Berhan M.N. Model development for mechanical properties and

- weld quality class of friction stir welding using multi-objective Taguchi method and response surface methodology. *J Mech Sci Technol.* 2015, 29, 2323–2331. <https://doi.org/10.1007/s12206-015-0527-x>
17. Ragavendran M., Chandrasekhar N., Ravikumar R., Saxena R., Vasudevan M., Bhaduri A.K. Optimization of hybrid laser – TIG welding of 316LN steel using response surface methodology (RSM). *Opt. Laser Eng.* 2017, 94, 27–36. <https://doi.org/10.1016/j.optlaseng.2017.02.015>
  18. Oleiwi AA, Jilabi AS J. The effects of travel speed of tungsten inert gas cladding of tungsten carbide and nickel composites on the microstructure of stainless steel. *Advances in Science and Technology Research Journal.* 2024, 18(4), 177–90. <https://doi.org/10.12913/22998624/188642>
  19. Dak, G., Guguloth, K., Vidyarthi, R.S., Fydrych, D., Pandey, C. Creep rupture study of dissimilar welded joints of P92 and 304L steels. *Weld World.* 2024. <https://doi.org/10.1007/s40194-024-01757-x>
  20. Kumar, A., Guguloth, K., Pandey, S.M., Fydrych, D., Sirohi, S., Pandey, C. Study on microstructure-property relationship of inconel 617 Alloy/304L SS steel dissimilar welds joint. *Metall Mater Trans* 2023. A 54, 3844–3870. <https://doi.org/10.1007/s11661-023-07136-3>
  21. Tarng Y.S., Yang W.H., Juang S.C. The use of fuzzy logic in the taguchi method for the optimisation of the submerged arc welding process. *Int J Adv Manuf Technol.* 2000, 16, 688–694. <https://doi.org/10.1007/s001700070040>
  22. ASME. Qualification Standard for Welding and Brazing, An International Code of ASME Boiler and Pressure Vessel Committee on Welding and Brazing. USA, 2010.
  23. Benlamnouar MF, Bensaid N, Azzoug MO, Saadi T, Zidani M, Badji R. Optimization and evaluation of mechanical and electrochemical properties of ferritic stainless steel welding using Taguchi design. *KEM* 2024, 973, 61–72. <https://doi.org/10.4028/p-oqmgc5>
  24. Ananthakumar K., Rajamani D., Balasubramanian E., Paulo Davim J. Measurement and optimization of multi-response characteristics in plasma arc cutting of Monel 400 using RSM and TOPSIS. *Measurement* 2019, 135, 725–737. <https://doi.org/10.1016/j.measurement.2018.12.010>
  25. Benlamnouar M.F., Saadi T., Bensaid N., Goumine M., Touggui Y., Temmar M. Modelling and optimization of dissimilar welding between 304L and HSLA-X70 using response surface methodology. In: Durakbasa N.M., Gençyılmaz M.G. (eds) *Digital Conversion on the Way to Industry 4.0.* ISPR 2020. Lecture Notes in Mechanical Engineering. Springer, Cham, 2021. [https://doi.org/10.1007/978-3-030-62784-3\\_39](https://doi.org/10.1007/978-3-030-62784-3_39)
  26. ASTM International. Standard Test Methods for Tension Testing of Metallic Materials. American National Standard, E8/E8M, 2010.
  27. Chen H., Huang J., Xia J., Zhao X., Lin S. Influence of processing parameters on the characteristics of stainless steel/copper laser welding. *J. Mater. Process. Technol.* 2015, 222, 43–51. <https://doi.org/10.1016/j.jmatprotec.2015.03.003>
  28. Meng Y., Li X., Gao M., Zeng X. Microstructures and mechanical properties of laser-arc hybrid welded dissimilar pure copper to stainless steel. *Opt. Laser Technol.* 2019, 111, 140–145. <https://doi.org/10.1016/j.optlastec.2018.09.050>